

Received February 9, 2018, accepted March 4, 2018, date of publication March 12, 2018, date of current version April 18, 2018.

Digital Object Identifier 10.1109/ACCESS.2018.2815043

# Teaching, Analyzing, Designing and Interactively Simulating Sliding Mode Control

**RAMON COSTA-CASTELLÓ<sup>1,2</sup>, (Senior Member, IEEE), NILIANA CARRERO<sup>2</sup>, SEBASTIÁN DORMIDO<sup>3</sup>, (Member, IEEE), AND ENRIC FOSSAS<sup>2</sup>, (Member, IEEE)**

<sup>1</sup>Institut de Robòtica i Informàtica Industrial, Universitat Politècnica de Catalunya, 08028 Barcelona, Spain

<sup>2</sup>Automatic Control Department (ESAI), Universitat Politècnica de Catalunya (UPC), 08034 Barcelona, Spain

<sup>3</sup>Departamento de Informática y Automática, Universidad Nacional de Educación a Distancia, 28015 Madrid, Spain

Corresponding author: Ramon Costa-Castelló (ramon.costa@upc.edu)

This work was supported in part by the Spanish Ministry of Economy and Competitiveness (MINECO/FEDER) under Project DPI2012-31303 and Project DPI2015-69286-C3-2-R, in part by the Spanish State Research Agency through the María de Maeztu Seal of Excellence to IRI under Grant MDM-2016-0656, and in part by the AGAUR of Generalitat de Catalunya through the Advanced Control Systems (SAC) Group under Grant 2017 SGR 482.

**ABSTRACT** This paper introduces an interactive methodology to analyze, design, and simulate sliding model controllers for  $\mathbb{R}^2$  linear systems. This paper reviews sliding mode basic concepts and design methodologies and describes an interactive tool which has been developed to support teaching in this field. The tool helps students by generating a nice graphical and interactive display of most relevant concepts. This fact can be used so that students build their own intuition about the role of different parameters in a sliding mode controller. Described application has been coded with Sysquake using an event-driven solver technique. The Sysquake allows using precise integration methods in real time and handling interactivity in a simple manner.

**INDEX TERMS** Sliding mode control, interactive simulations, control education.

## I. INTRODUCTION

Sliding Modes based Control (SMC) is becoming a very used technique in recent times. It has been applied in different fields such as, among others, power electronics [1], magnetic levitation systems [2] or electromechanical systems [3], [4]. The reasons can be found in the robustness offered against uncertainty and disturbances in both linear and non-linear systems. Therefore, this technique is increasingly being included in university studies, especially in Masters.

The key idea behind SMC is imposing a closed-loop dynamics of lower order than that of the plant, which defines a surface in the original state space. The control policy is based on switching between two predefined values accordingly to the surface side where the system is in each instant of time [5]–[8].

The analysis of SMC is usually based on differential geometric ideas and other sophisticated mathematical concepts. Consequently, many students have difficulties in assimilating SMC principles, in particular those who do not have strong mathematical background, which is the case in most engineering studies at present. Fortunately, most SMC principles have a nice geometric visualization. A way to support students learning is taking profit from these graphical representations.

Nowadays, computers offer great graphical and computational capabilities, even mobile phones and tablets can produce nice figures obtained after computer simulations. Visualization is a very relevant sense which contributes to build intuition and attract students attention in a given topic and help them to improve their understanding of difficult concepts [9]–[14]. Although nice graphical representations are a very important pedagogical tool which has been exploited by teachers from old times, current computers allow to build dynamic graphical representations which are updated in real-time taking into account the user activity. This allows interactivity to enter the scene.

Interactivity has proven to be a very important way humans use to improve their knowledge about the environment. Engineering and control education, in particular, are also trying to take profit from it to improve learning mechanism; consequently, interactivity is one of most relevant concepts which is being exploited in control education nowadays [15], [16]. Some examples are, the Interactive Learning Modules [13], [17] or FreePIDTools [18] which were designed to introduce students to PID control, SISO-QFTIT (Robust QFT based control) or LCSD (Linear Control System Design) which have been introduced to interactively design robust control systems [9], SISO-GPCIT and MIMO-GPCIT [11] which have been used to introduce students to Generalized

Predictive Control, ITTSAE is a set of interactive tools designed to analyze Time Series [19], also dead-time compensators have been analyzed using interactive methods [20] between others. Similarly, several introductory control books are distributed jointly with a set of graphical and interactive applications to illustrate most relevant concepts [21] [12], [22] [23].

This paper describes a methodology to introduce students to the analysis and design of SMC for  $\mathbb{R}^2$  linear systems. The methodology is supported with a graphical and interactive tool which can be used by the professor in his lectures in order to transform static drawings in slides or blackboard into attractive figures updated in real-time. Interactivity allows to visualize cause-effect relations when modifying controller parameters. Additionally, the students can use the tool during self-study or to solve homework exercises proposed by the professor.

One of the main characteristics of SMC is that the control action is discontinuous, as it switches between two different values. This kind of systems cannot be solved efficiently using regular solvers [24]. An accurate resolution would require to use very small simulation steps so that switching times are obtained with precision. Since this approach makes interactively simulating almost impossible, an event-based integration [14], [24] is used in this work. Modern versions of simulation tools have capabilities to implement this type of solving method. Tools like MATLAB [25], Easy Java Simulations (EJS) [26] and Sysquake [27] are concrete examples. EJS has been previously used to simulate systems containing SMC controllers [14]. Differently, in this work Sysquake has been used to take profit from its improved visualization methods and its efficient solvers which allow to perform highly interactive simulations with an attractive and appealing visualization.

SMC is a nonlinear control methodology, consequently and differently from linear control systems, concepts like initial conditions and region of attraction [28] play a very important role; unfortunately computing the region of attraction is not a simple issue in the general case. In this paper an original methodology to compute the region of attraction of the system is developed. This methodology has been implemented in the described tool.

The paper is organized as follows. Section II introduces most relevant concepts used to design and analyze sliding mode controllers for linear planar systems. Section III describes how the application has been implemented and its main functionalities. Section IV contains two examples showing how the application is used to analyze given problems. Finally, some conclusions about this work are included in Section VI.

## II. SLIDING MODE CONTROL IN PLANAR SYSTEMS

In this work we focus on 2D linear systems, which can be defined as

$$\dot{\mathbf{x}} = \mathbf{A}\mathbf{x} + \mathbf{b}u \quad (1)$$

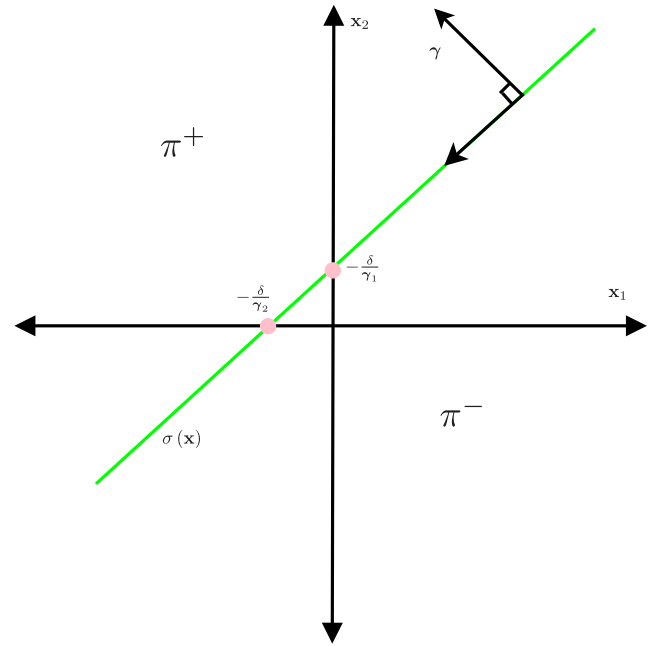


FIGURE 1. Linear sliding surface definition in the phase plane ( $x_1$ - $x_2$ ).

where  $\mathbf{x} \in \mathbb{R}^2$  is the state vector,  $u$  is the input,  $u \in \mathbb{R}$ ,  $\mathbf{A} \in \mathbb{R}^{2 \times 2}$  the state transition matrix and  $\mathbf{b} \in \mathbb{R}^{2 \times 1}$  the input vector. The solution of linear systems is well-known. Linear systems can be written using different realizations, each one of them offers equivalent ways to write the same system. In this work, for simplicity reasons and without loss of generality, matrix  $\mathbf{A}$  is written as

$$\mathbf{A} = \begin{pmatrix} 0 & 1 \\ a_{21} & a_{22} \end{pmatrix}, \quad (2)$$

where the components of the second row are the opposite sign of the coefficients of the characteristic polynomial, that is,  $C_A(\lambda) = \lambda^2 - a_{22}\lambda - a_{21}$ . The zeros of  $C_A(\lambda)$  are the eigenvalues of  $\mathbf{A}$ . These values define the shape of the solution of (1).

In conventional SMC, the control action,  $u$ , is a piecewise continuous action, i.e., the sign of an affine function:

$$u = \begin{cases} 1 & \text{if } \sigma(\mathbf{x}) > 0 \\ -1 & \text{if } \sigma(\mathbf{x}) < 0 \end{cases} \quad (3)$$

where  $\sigma(\mathbf{x})$ , is usually an affine function defined as

$$\sigma(\mathbf{x}) = \boldsymbol{\gamma}\mathbf{x} + \delta. \quad (4)$$

Note that  $\sigma(\mathbf{x}) = 0$  is a line,  $\boldsymbol{\gamma} = (\gamma_1, \gamma_2) \in \mathbb{R}^2$  is a normal vector to the line and  $\delta \in \mathbb{R}$  a scalar value to place the line over the plane (Figure 1).

As it can be seen from the definition, the control input  $u$  takes two values only. As a consequence, the dynamics (not the trajectories) are piecewise continuous. Furthermore, note that they are not defined on the line  $\sigma(\mathbf{x}) = 0$ . However, in some subsets of  $\sigma(\mathbf{x}) = 0$  trajectories chatter around

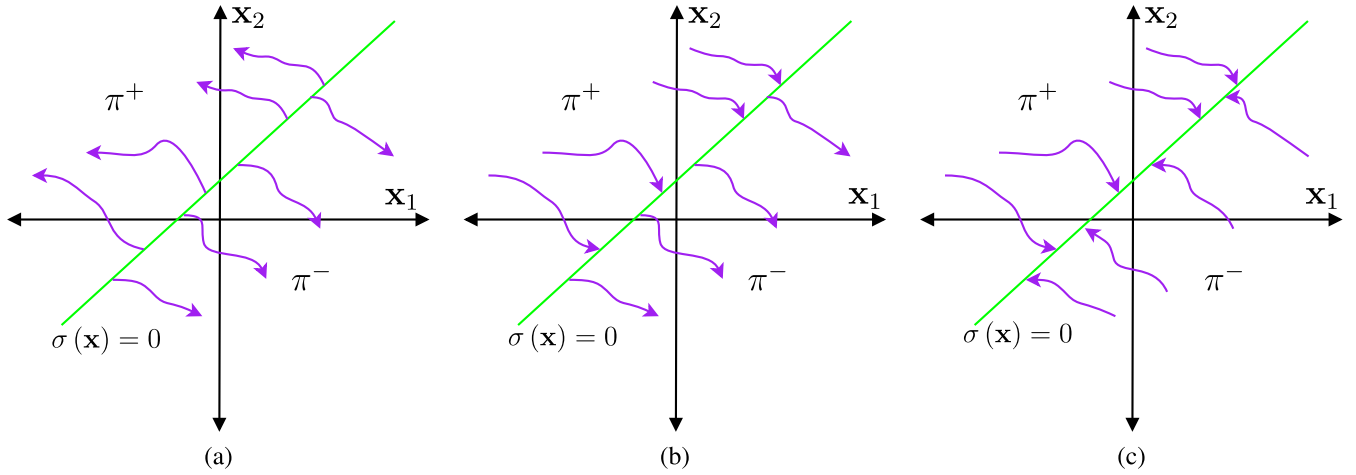


**FIGURE 2.** Different possible phase plots close to the switching surface: (a)  $\sigma(\mathbf{x}) = 0$  acts as a repeller, (b) trajectories cross  $\sigma(\mathbf{x}) = 0$  and (c)  $\sigma(\mathbf{x}) = 0$  acts as an attractor.

$\sigma(\mathbf{x}) = 0$  and, ideally, they evolve over the line. This kind of dynamics are referred to as *sliding modes* or *sliding regimes*.

In a more formal manner, it is said that there exists sliding regime in a subset  $R \subset \{\mathbf{x} \in \mathbb{R}^2 \mid \sigma(\mathbf{x}) = 0\}$ , if there exists a neighborhood  $\mathcal{O}$  of  $R$  in  $\mathbb{R}^2$  such that all trajectories starting in  $\mathcal{O}$  converge to  $R$  and remain in it. If finally, the trajectories leave  $R$ , they do it through the border  $\partial R \subset \{\mathbf{x} \in \mathbb{R}^2 \mid \sigma(\mathbf{x}) = 0\}$ .

#### A. SLIDING REGIME CONDITIONS

At this point, two natural questions arise:

- Under which conditions do sliding modes exist?
- Presuming that sliding modes exist, what dynamics do they fulfill?

In this section the sliding regime existence problem for the system defined by (1), (3) and (4) is studied. The line defined by  $\sigma(\mathbf{x}) = 0$  in (4) decomposes  $\mathbb{R}^2$  in two half-planes (Figure 1):

$$\begin{aligned}\pi^- &= \{\mathbf{x} \in \mathbb{R}^n \mid \sigma(\mathbf{x}) < 0\} \\ \pi^+ &= \{\mathbf{x} \in \mathbb{R}^n \mid \sigma(\mathbf{x}) > 0\}.\end{aligned}$$

According to the control input, (3), different vector fields act on  $\pi^-$  and  $\pi^+$ . These vector fields are  $\mathbf{f}^-$  and  $\mathbf{f}^+$ , respectively, and they are defined by  $\mathbf{f}^- = \mathbf{Ax} - \mathbf{b}$  and  $\mathbf{f}^+ = \mathbf{Ax} + \mathbf{b}$ . Both  $\mathbf{f}^-$  and  $\mathbf{f}^+$  are smooth vector fields on all  $\mathbb{R}^2$ . Figure 2 shows different dynamics close to  $\sigma(\mathbf{x}) = 0$  depending on the relative position of  $\mathbf{f}^-$  and  $\boldsymbol{\gamma}$ , and  $\mathbf{f}^+$  and  $\boldsymbol{\gamma}$ . In Figure 2.a, trajectories leave  $\sigma(\mathbf{x}) = 0$ , which acts as a repeller; in Figure 2.b, trajectories cross  $\sigma(\mathbf{x}) = 0$ ; finally, in Figure 2.c, trajectories point forward  $\sigma(\mathbf{x}) = 0$ , which acts as an attractor. Sliding modes take place in the last case.

The time derivative of  $\sigma$  over the trajectories can be computed as:

$$\dot{\sigma} = \frac{\partial \sigma}{\partial \mathbf{x}} \dot{\mathbf{x}}.$$

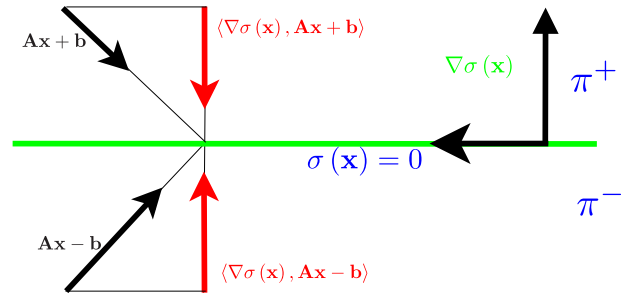


**FIGURE 3.** Vector fields direction around the sliding surface when a sliding regime exists.

Usually the scalar product is noted as  $\langle \cdot, \cdot \rangle$  and the gradient vector  $\nabla \sigma \triangleq \frac{\partial \sigma}{\partial \mathbf{x}}$ . Using this notation time derivative of  $\sigma$  over the trajectories can be written as:  $\dot{\sigma} = \langle \nabla \sigma, \dot{\mathbf{x}} \rangle$ . For the sliding surface defined in (4),  $\nabla \sigma = \boldsymbol{\gamma}$  while  $\dot{\mathbf{x}}$  will be  $\mathbf{f}^-$  in  $\pi^-$  and  $\mathbf{f}^+$  in  $\pi^+$ .

A necessary and sufficient condition for the existence of a sliding regime in a subset  $R$  of  $\sigma(\mathbf{x}) = 0$  is that  $\dot{\sigma} < 0$  when  $\sigma > 0$  and that  $\dot{\sigma} > 0$  when  $\sigma < 0$  [7]. These conditions guarantee that the system trajectories converge to  $\sigma(\mathbf{x}) = 0$ , i.e. the sliding surface acts an attractor (Figure 2.c).

Consequently, for the case of (1), (3) and (4), a sufficient condition for the existence of a sliding regime in a subset  $R$  of  $\sigma(\mathbf{x}) = 0$  is given by:

$$\langle \boldsymbol{\gamma}, \mathbf{f}^- \rangle > 0 \quad \text{and} \quad \langle \boldsymbol{\gamma}, \mathbf{f}^+ \rangle < 0. \quad (5)$$

Figure 3 shows an schematic representation of these conditions. Note that thanks to  $\mathbf{f}^-$ ,  $\mathbf{f}^+$  and  $\sigma(\mathbf{x}) = 0$  are smooth, inequalities in (5) hold in a neighborhood of  $R$ .

#### B. SLIDING MODE EXISTENCE AND IDEAL SLIDING DYNAMICS

In order to analyze the closed-loop behavior it is necessary to understand the dynamics in sliding modes. Two different

methods to address this issue can be found in the literature: Filippov approach [29], and the equivalent control method introduced by V. Utkin [7].

Filippov approach defines the dynamics at a given point  $\mathbf{x} \in R$  as the intersection between the convex hull spanned by  $\mathbf{f}^-$  and  $\mathbf{f}^+$  with the tangent manifold to  $\sigma(\mathbf{x}) = 0$  at  $\mathbf{x}$ ; in our particular case,  $\sigma(\mathbf{x}) = 0$  itself. The equivalent control approach defines the equivalent control as the required control action that makes  $R$  flow-invariant (i.e. trajectories starting in  $R$  remain in  $R$ ). Both approaches provide the same solution in affine systems as the ones we deal with. The main theoretical results in this section will be presented using the equivalent control approach.

Let assume that for  $t \geq t_0$  the system is in sliding regime, i.e.,  $\sigma(\mathbf{x}(t)) = 0$ , and remains in it during a time interval  $t \in [t_0, t_0 + \varepsilon)$ . During this interval  $\sigma(\mathbf{x}(t)) = 0$  and  $\frac{d\sigma(\mathbf{x}(t))}{dt} = 0$  as well. The latter equation allows obtaining the equivalent control, i.e., a continuous control action that forces trajectories of (1) to remain in  $\sigma(\mathbf{x}(t)) = 0$ . Namely,

$$0 = \frac{d\sigma(\mathbf{x}(t))}{dt} = \langle \nabla \sigma, \dot{\mathbf{x}} \rangle = \langle \nabla \sigma, \mathbf{A}\mathbf{x} + \mathbf{b}u_{eq} \rangle \quad (6)$$

then,

$$u_{eq}(\mathbf{x}) \triangleq -\frac{\langle \nabla \sigma, \mathbf{A}\mathbf{x} \rangle}{\langle \nabla \sigma, \mathbf{b} \rangle}. \quad (7)$$

Equation (7) yields a necessary condition for the existence of  $u_{eq}$ . Namely,

$$\langle \nabla \sigma, \mathbf{b} \rangle \neq 0. \quad (8)$$

It is named *transversality condition* and it states that the vector field  $\mathbf{b}$  should not be tangent to the sliding surface. This is equivalent to require for the system (1) with output (4) to be relative degree 1.

Transversality condition is a necessary and sufficient condition for sliding modes to exist if there are no constraints on  $u$ . If (8) holds, but (5) does not,  $\sigma(\mathbf{x})$  should be replaced by  $-\sigma(\mathbf{x})$ .

The equivalent control,  $u_{eq}(\mathbf{x})$ , corresponds to a continuous ideal control action which would produce the same results than the switching control law, (3), once the sliding regime is achieved. As the control action, (3), is bounded the achievable equivalent control action will also be bounded [5], [7]:

$$-1 < u_{eq}(\mathbf{x}) < 1. \quad (9)$$

Consequently, (9) becomes a necessary and sufficient for the sliding regime existence and it can be used to obtain the sliding domain on  $\sigma(\mathbf{x}) = 0$ ,  $R$ .

The dynamics on  $R$  (ideal sliding dynamics) can also be given by

$$\begin{aligned} \dot{\mathbf{x}} &= \mathbf{A}\mathbf{x} + \mathbf{b}u_{eq} \\ 0 &= \sigma(\mathbf{x}) \end{aligned} \quad (10)$$

which leads to a first-order dynamics on the switching line.

One of the main tasks in SMC is to define a sliding surface  $\sigma(\mathbf{x}) = 0$  so that the closed-loop system (1)-(3)-(4) fulfills given specifications.

### C. DESIGN HINTS

As previously stated, ideal sliding dynamics can be defined by (10). Although this expression is complete, it is difficult to use it to design the switching surface. An alternative approach already mentioned is to manipulate (10) in order to obtain the dynamics in terms of  $\mathbf{x}_1$  or  $\mathbf{x}_2$ . Under the assumption that  $\gamma_2 \neq 0$ ,  $\sigma(\mathbf{x}(t)) = 0$  can be solved for  $\mathbf{x}_2$ , the line can be parametrized by  $\mathbf{x}_1$ , and the sliding dynamics can be defined through  $\mathbf{x}_1$  only.

If  $a_2 \neq 0$ ,<sup>1</sup> (10) is equivalent to

$$\dot{\mathbf{x}}_1 = \beta_{11}\mathbf{x}_1 + \beta_{12} \quad (11)$$

or alternatively, equivalent to:

$$\dot{\mathbf{x}}_2 = \beta_{21}\mathbf{x}_2 + \beta_{22} \quad (12)$$

where  $\beta_{ij}$  are values depending on the switching line and the system parameters. Using the switching surface parameters as design parameters it is possible to set  $\beta_{ij}$  to the desired values, which results in setting the sliding dynamics.

Another approach is to encompass the problem of regulating an output defined by

$$y = \rho\mathbf{x} \quad (13)$$

to a desired value,  $y_{ss}$ , by designing an appropriate switching line that will depend on the output relative degree. Two cases must be distinguished.

- $\rho\mathbf{b} \neq 0$  (relative degree 1). In this case, it is possible to set the value of  $y$  to  $y_{ss}$ , i.e.  $y = y_{ss}$ . Take  $\gamma = \rho$  and  $\delta = -y_{ss}$  as surface parameters. Whenever the ideal sliding dynamics is stable, we will achieve  $y = y_{ss}$ . Note that this method does neither allow to determine the ideal sliding dynamics nor its stability, they can be computed through the equivalent control method.
- $\rho\mathbf{b} = 0$  and  $\rho\mathbf{A}\mathbf{b} \neq 0$  (relative degree 2). In this case, it is possible to impose the following output dynamics:

$$\tau\dot{y} + y = y_{ss}. \quad (14)$$

Which in the original coordinate system becomes  $\gamma = \tau\rho\mathbf{A} + \rho$  and  $\delta = -y_{ss}$ .

### D. REGION OF ATTRACTION

Conditions under which sliding regimes exist were analyzed in the previous section. Unfortunately, deduced conditions are local and only provide relevant information in a region close to the sliding surface. This information might not be enough in practical applications. Furthermore, it is difficult to obtain an analytical criterion which allows to determine the basin of attraction of  $R$ , i.e., the initial conditions of those trajectories that impact on  $R$  in finite time.

These attraction regions are of great relevance from a practical point of view. Let us define

$$\eta^- = \{\mathbf{x}_0 \in \pi^- | \mathbf{x}(0) = \mathbf{x}_0, \dot{\mathbf{x}} = \mathbf{f}^-, \exists t > 0 | \mathbf{x}(t) \in R\} \quad (15)$$

<sup>1</sup>If  $a_2 = 0$  only certain parametrizations might be applicable.

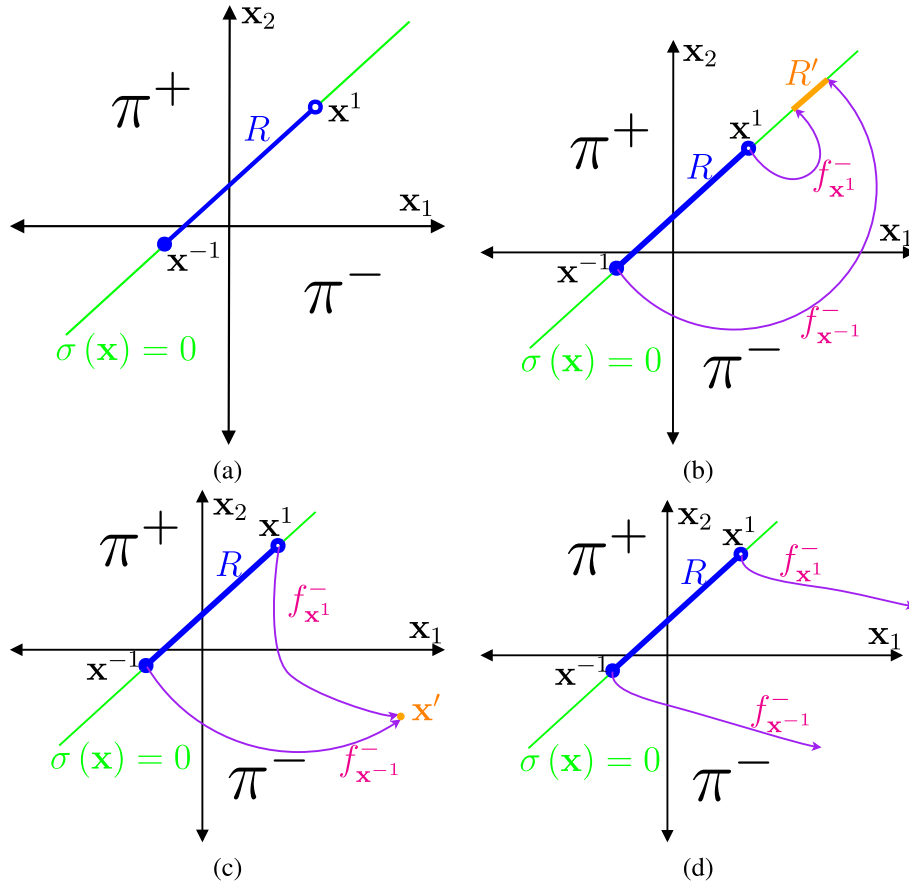


**FIGURE 4.** Attraction zone components. (a)  $R$  is always a component of the attraction zone boundary, its limits are  $\mathbf{x}^1$  and  $\mathbf{x}^{-1}$ ; (b) in some cases  $f_{\mathbf{x}^1}^-$  and  $f_{\mathbf{x}^{-1}}^-$  intersect  $\sigma(\mathbf{x}) = 0$ ; (c) in some cases  $f_{\mathbf{x}^1}^-$  and  $f_{\mathbf{x}^{-1}}^-$  converge to point in  $\mathbf{x}' \in \pi^-$ ; (d) in some cases  $f_{\mathbf{x}^1}^-$  and  $f_{\mathbf{x}^{-1}}^-$  tend to infinite without intersecting  $\sigma(\mathbf{x}) = 0$ .

$$\eta^+ = \{\mathbf{x}_0 \in \pi^+ | \mathbf{x}(0) = \mathbf{x}_0, \dot{\mathbf{x}} = \mathbf{f}^+, \exists t > 0 | \mathbf{x}(t) \in R\}. \quad (16)$$

$\eta = \eta^- \cup \eta^+$  is a subset of the basin of attraction of  $R$ . In particular, it corresponds to the region of attraction that generates a sliding regime after hitting the switching surface once.

Computing the attraction zone might not be an easy problem. Fortunately, computing its boundaries,  $\partial\eta^-$  and  $\partial\eta^+$ , might be easier. These boundaries are composed of solutions to (1)-(3)-(4) [28] and can be decomposed in different components that will be analyzed below. For simplicity reasons the analysis is only described for  $\partial\eta^-$ . The reasoning would be exactly the same for the case of  $\partial\eta^+$ .

The boundary of  $\eta^-$ ,  $\partial\eta^-$ , is composed of the following components:

- $R$ , which is a line segment, a subset of  $\sigma(\mathbf{x}) = 0$ . Its boundary can be obtained by combining the sliding surface equation, and the equivalent control limits,  $u_{eq}(\mathbf{x}) = 1$  and  $u_{eq}(\mathbf{x}) = -1$ , respectively. This boundary consists of two points:  $\mathbf{x}^1$  and  $\mathbf{x}^{-1}$  (see Figure 4.a).
- $f_{\mathbf{x}^1}^-$ ,  $f_{\mathbf{x}^{-1}}^-$ , which are two trajectories reaching  $\mathbf{x}^1$  and  $\mathbf{x}^{-1}$  from  $\pi^-$ . These trajectories can be obtained by

evaluating  $\dot{\mathbf{x}} = \mathbf{f}^-$  with  $\mathbf{x}(0) = \mathbf{x}^1$  and  $\mathbf{x}(0) = \mathbf{x}^{-1}$ , respectively, in backwards times. These curves can be analytically obtained by evaluating the linear system solution.

The relation between these two curves and  $\partial\eta^-$  can take different forms:

- $f_{\mathbf{x}^1}^-$  and  $f_{\mathbf{x}^{-1}}^-$  intersect  $\sigma(\mathbf{x}) = 0$ . In this case, only a segment of  $f_{\mathbf{x}^1}^-$  and  $f_{\mathbf{x}^{-1}}^-$  belongs to the boundary and a segment of  $\sigma(\mathbf{x}) = 0$ ,  $R'$ , closes the boundary (see Figure 4.b).

This structure appears when the eigenvalues of  $\mathbf{A}$  belong to  $\mathbb{C}$ ,  $-\mathbf{A}$  has eigenvalues on  $\mathbb{C}^+$  or  $-\mathbf{A}$  has all its eigenvalues in  $\mathbb{C}^-$ , and the equilibrium point of  $\dot{\mathbf{x}} = -\mathbf{A}\mathbf{x} - \mathbf{b}$ ,  $-\mathbf{A}^{-1} \cdot \mathbf{b}$  belongs to  $\pi^+$ .

- $f_{\mathbf{x}^1}^-$  and  $f_{\mathbf{x}^{-1}}^-$  tend to a finite point,  $\mathbf{x}' \in \pi^-$ , as  $t \rightarrow -\infty$  (see Figure 4.c).

This structure appears when the eigenvalues of  $-\mathbf{A}$  belong to  $\mathbb{C}^-$  and the equilibrium point of  $\dot{\mathbf{x}} = -\mathbf{A}\mathbf{x} - \mathbf{b}$ ,  $\mathbf{x}' = -\mathbf{A}^{-1} \cdot \mathbf{b}$  belongs to  $\pi^-$ .

- $f_{\mathbf{x}^1}^-$  and  $f_{\mathbf{x}^{-1}}^-$  tend to infinite as  $t \rightarrow -\infty$  (see Figure 4.d).

This structure appears when  $-\mathbf{A}$  has real eigenvalues in  $\mathbb{C}^+$ .



- Line segments: when the eigenvalues of  $-\mathbf{A}$  are real, its eigenvectors define a decomposition of  $\mathbb{R}^2$ . This decomposition is defined by lines intersecting in the equilibrium point,  $\mathbf{A}^{-1}\mathbf{b}$ , and aligned with the eigenvectors directions. These lines are, in some cases, part of  $\partial\eta^-$ .

Combining all these components and computing its intersections it is possible to build  $\partial\eta^-$  for each particular case.

### III. VARIABLE STRUCTURE SYSTEM INTERACTIVE SIMULATION

Developing an interactive application that analyzes the behavior of systems defined by (1)-(3) implies solving a discontinuous set of differential equations. Using a regular ODE solver to address this problem implies using very small discretization intervals, which leads to a slow simulation. In addition, this approach may generate erroneous results.<sup>2</sup> In order to obtain the results in a time which allows interactivity and assures correct results another approach must be used.

An approach to solve (1)-(3) in an efficient and correct manner is to identify the different continuous dynamics appearing in the system, solve those latter using regular methods, and switch between them at proper time instants. This approach is usually named *event-based simulation* [24]. This methodology will be used in the development of the simulation environment described in this work. It has already been used to simulate hybrid systems [30] and systems with complex sliding regimes [31].

In this work, Sysquake [27] has been used as development tool. This software supports *event-based simulation*, by defining the vector field functions, *state events* detection function, and *state events* management function. The vector field function defines the vector field that must be integrated in each time, depending on the value of a configuration variable; the state event detection function corresponds to a function which equals 0 when an event is reached; finally the *state events* management function is called when an event is detected, this function determines which is the next set of equations to be used by fixing the configuration variable value. All these functions are integrated in single integration procedure.

The system (1)-(3), contains three different continuous regimes:

- 1) The system is moving in  $\pi^-$ , in this configuration the vector field to be solved is defined by  $\mathbf{f}^-$ .
- 2) The system is moving in  $\pi^+$ , in this configuration the vector field to be solved is defined by  $\mathbf{f}^+$ .
- 3) The system is moving over  $R$ , in this configuration the vector field to be solved is defined by (10).

It is important to state that differently from the two previous cases, (10) leads to a Differential Algebraic Equation system (DAE). To solve these equations a DAE solver [32] is needed. Unfortunately, Sysquake has not such a solver.

<sup>2</sup>This may be important when the system is in a sliding regime.

Solving

$$\dot{\mathbf{x}} = \mathbf{A}\mathbf{x} + \mathbf{b} \cdot u_{eq}(\mathbf{x}) \quad (17)$$

with appropriate initial conditions ( $\sigma(\mathbf{x}) = 0$ ) would be ideally enough. Unfortunately, when solved with a real ODE solver, the solution trajectory would diverge from the switching surface after sometime due to numerical problems. To avoid this problem a regularization scheme is used [31], i.e. equation (17) is replaced by the following one:

$$\dot{\mathbf{x}} = \mathbf{A}\mathbf{x} + \mathbf{b} \cdot u_{eq} + \gamma \cdot \sigma(\mathbf{x}) \cdot \left( \frac{\partial \sigma(\mathbf{x})}{\partial \mathbf{x}} \right)^T \quad (18)$$

The new system is equal to (17) with the addition of a regularization term, composed by the product of a vector normal to the switching surface, the switching surface and a scalar term to be tuned. The solution of (18) is exactly the same than that of (17) when the trajectory is over the switching surface. When the trajectory drifts from the surface a component appears which takes the trajectory back to the switching surface.

This procedure allows to obtain the solution of (10) with a regular ODE solver and without increasing too much the complexity of the equations to be solved.

In order to determine when the solver needs to change from one vector field to another, it is necessary to determine when the trajectory moves from  $\pi^-$  to  $\pi^+$  or  $R$  and viceversa. These transitions can be related with a set of events:

- 1) The trajectory hits the switching surface, i.e.,  $\sigma(\mathbf{x}) = 0$ .
- 2) The equivalent control reaches its limit  $u_{eq}(\mathbf{x}) = 1$  or  $u_{eq}(\mathbf{x}) = -1$ . These two cases can be integrated in a single function, i.e.,  $|u_{eq}(\mathbf{x})| = 1$ .

Both events are mutually excluding, consequently only one event must be detected at each time. Once an event is detected, it is possible to uniquely determine the following state from the previous state, the detected concrete event and the value of  $\mathbf{x}$ . Figure 5 shows the flow diagram used to obtain the system trajectories.

Following the described methodology, an interactive tool named SMCITool (Sliding Mode Control Interactive Tool) has been designed and implemented to be used to illustrate most relevant concepts in sliding mode control. SMCITool can be downloaded from :

<https://sites.google.com/site/ramoncostacastello/smcitool>

Figure 6 shows the complete view of the application. The interface is composed of four main blocks: the upper left (**Textual definition**) one allows to describe the plant ( $\mathbf{A}, \mathbf{b}$ ) and the sliding surface both using a graphical or textual approach; the lower left part (**Control action, states and output evolution**) shows the evolution of most relevant closed-loop variables (control action,  $u$ , states  $\mathbf{x}$  and output,  $y$ ); the upper right part (**Event evolution**) contains a time diagram describing the events that are generated during the simulation; and finally, the lower right part (**Closed-loop phase plane**) contains a phase diagram that shows

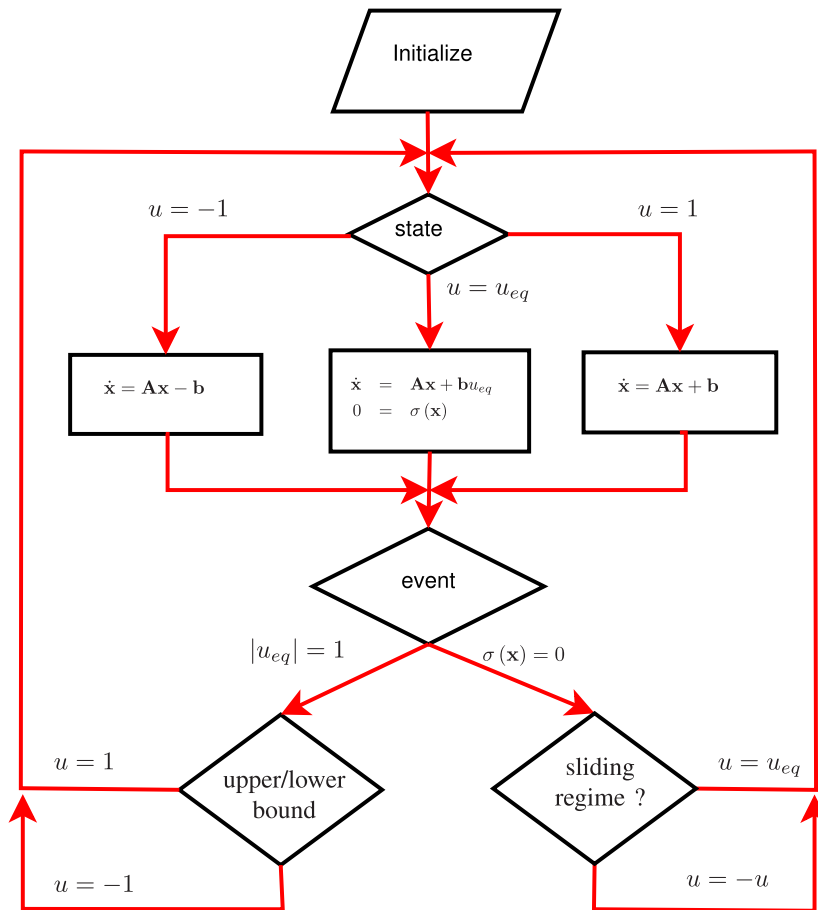


FIGURE 5. Event-based simulation structure used to simulate the closed-loop system.

the sliding surface,  $\sigma(\mathbf{x}) = 0$ , the trajectory starting at a given initial condition, the flow lines and the attraction zones. All the elements are interactive and are updated in real time.

In the following, the main functionalities of each part will be described:

- Textual definition: In this section it is possible to define the sliding surface and the system using text fields or sliders. Using a check button it is possible to select between three possibilities:
  - Output: The components of  $\rho$ , (13),  $y_{ss}$  and  $\tau$ , (14), can be defined. For relative degree 2 outputs, also the value of  $\tau$ , (14), can be defined. From these values, the values of  $\gamma$  and  $\delta$ , (4), are automatically computed.
  - Surface: The values of  $\gamma$  and  $\delta$ , (4), can be defined using text fields or sliders.
  - Model: The eigenvalues of  $\mathbf{A}$  and the values of the components of  $\mathbf{b}$  can be introduced using textfields and sliders.

In the bottom of this section there exist two buttons, one named “start” and the other named “stop”. When pressing the start button, an animation which moves

a circle over the trajectory begins. The evolution of the circle over the trajectory is proportional to the simulation time (takes 10s to move from the initial conditions to the last point). When the circle reaches the last point, the animation automatically begins again until the stop button is pressed or any other interactive element is modified.

- Graphical definition: In this part a complex plane is shown, over it the eigenvalues of  $\mathbf{A}$  (red crosses) and the components of  $\mathbf{b}$  (red circle) are shown. Both elements can be modified by dragging them. Over this complex plane the equivalent dynamic pole is shown (green cross). This is presented only if a sliding regime exist.
- Control action, states and output evolution: This part is divided in two figures. The upper one represents the control action. When the trajectories are over a sliding regime the equivalent control is shown. The lower one can display the state variables ( $\mathbf{x}_1, \mathbf{x}_2$ ) and the output ( $y$ ) against time. Also the Ideal dynamics (the one defined over the switching surface by  $y_{ss}$  and  $\tau$  in (14)) is also shown, for the state variables and the output. Over the output, two control points (gray circles)

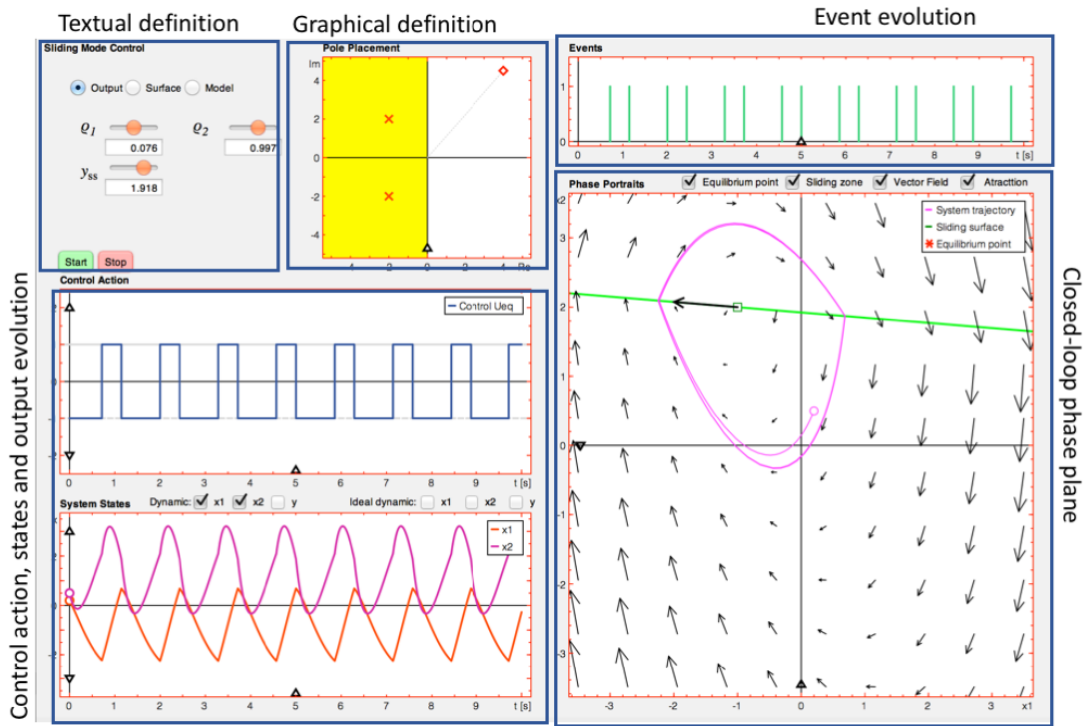


**FIGURE 6.** SMCITool: Application components. The view shows a case where no sliding regime exists. The closed-loop system describes a limit cycle. The systems trajectories are continuously moving from  $\pi^-$  to  $\pi^+$ .

are included to interactively define  $\tau$  and  $y_{ss}$  respectively.

- Event evolution: This part shows the time instant for which an event is generated during the simulation. Different colors are used for different events types. A green bar is used to visualize hitting the switching surface without entering in a sliding regime, a blue bar is used to visualize hitting the switching surface entering in a sliding regime and a light blue bar is used to visualize the ending of a sliding regime.
- Closed-loop phase plane: This figure contains the trajectory (pink curve) which the closed-loop system describes over the phase plane (defined by  $x_1$ - $x_2$ ). The initial conditions (pink circle) can be interactively modified by dragging them. The switching surface is drawn in green. This line can be interactively modified by dragging it, it can be rotated over a control point (small green square). Along the switching surface a black arrow line which corresponds to  $\gamma$ . The control point can also be modified by dragging it to the desired point.

Finally, the figure upper part contains several check button that can be used to customize the figure:

- Equilibrium point: when it is active the closed-loop equilibrium point is drawn (red star). This equilibrium point may be stable or unstable and might be inside our outside  $R$ .
- Sliding zone: when this option is active the region where sliding regime exist,  $R$ , is drawn in blue.

- Vector field: when this option is active different arrows showing the vector field direction are shown over the phase plane.
- Attraction: when this option is active the region of attraction,  $\eta$ , is shown over the phase plane.

Many figures contain black triangles which can be used to change the scale.

It is important to note that due to the interactivity all the information is automatically updated when any change is applied.

#### IV. EXAMPLES

##### A. EXAMPLE 1

System (1) is defined by:

$$\mathbf{A} = \begin{pmatrix} 0 & 1 \\ -4.25 & -1 \end{pmatrix} \quad \mathbf{b} = \begin{pmatrix} 0 \\ -5 \end{pmatrix}.$$

The control goal is to regulate the value of the output :

$$y = \mathbf{x}_1 = (1, 0)\mathbf{x} = \rho\mathbf{x}$$

to  $y_{ss} = 0.75$ .

As  $\rho\mathbf{b} = 0$ , the output relative degree is two. Consequently, it is possible to impose a convergence dynamics once the sliding regime is achieved:

$$\tau \frac{dy}{dt} + y = y_{ss}, \quad (19)$$

Note that  $\frac{dy}{dt} = \mathbf{x}_2$ , the sliding surface becomes:

$$\tau \cdot \mathbf{x}_2 + \mathbf{x}_1 = y_{ss}. \quad (20)$$



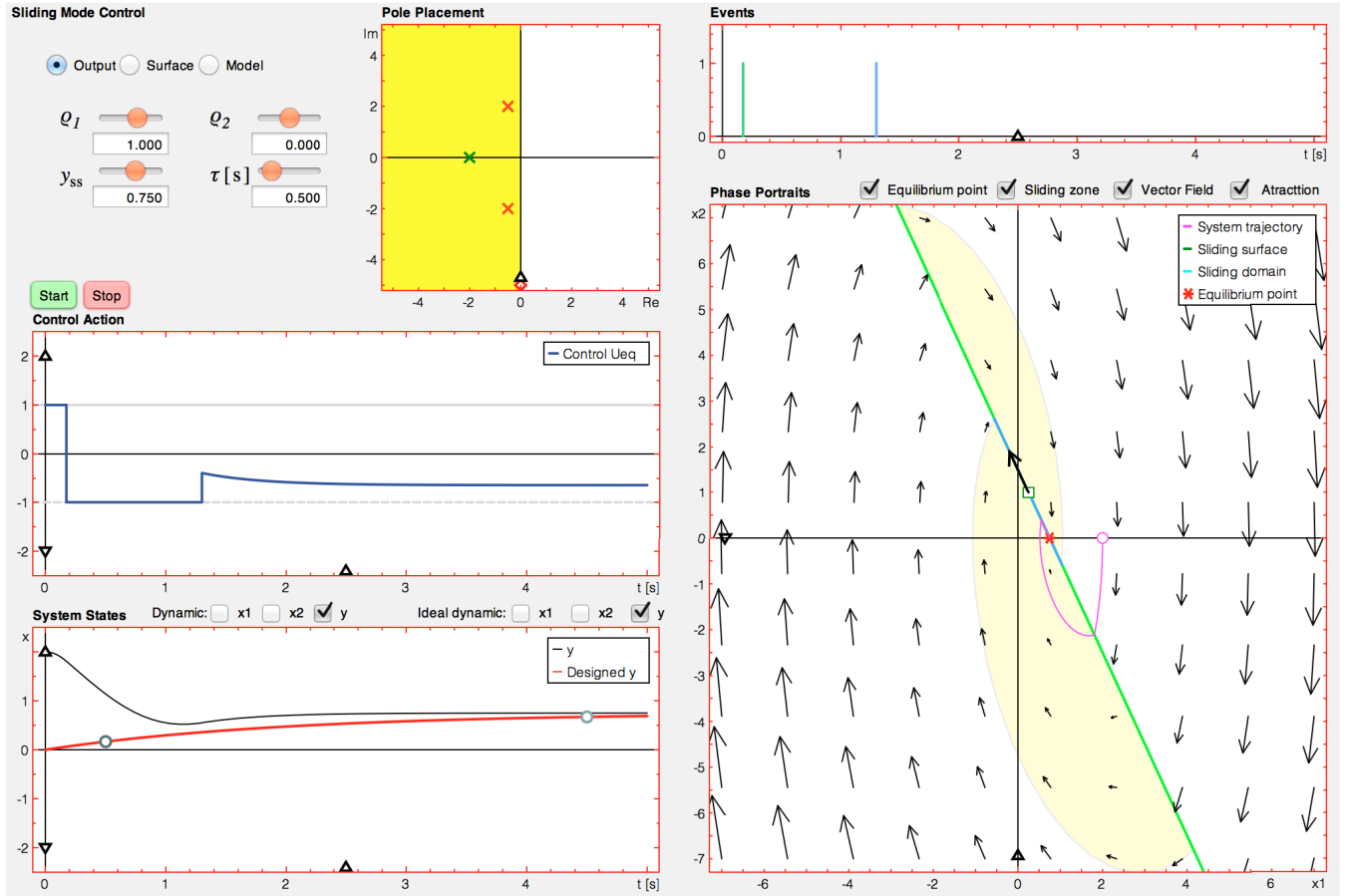


**FIGURE 7.** SMCITOOL: The view shows the case described in Example 1 for  $y_{ss} = 0.75$ . Trajectory begins in  $\pi^+$ , hits the sliding surface and enters  $\pi^-$ ; after some time it hits the sliding surface again and then enters the sliding regime. As the dynamics over the sliding surface is stable (the pole can be seen in green in the pole placement section) and the equilibrium point is in  $R$ , the output tends asymptotically to  $y_{ss}$ .

Which can be rewritten as:

$$\sigma(\mathbf{x}) = \boldsymbol{\gamma} \cdot \mathbf{x} - y_{ss} \quad (21)$$

where  $\boldsymbol{\gamma} = [1, \tau]$ . At this point  $\tau$  is selected as 0.5 s.

In order to analyze the closed-loop behavior, firstly the transversality condition is validated:

$$\langle \nabla \sigma, \mathbf{b} \rangle = -5\tau \neq 0.$$

Consequently, a sliding regime might exist. Secondly, the equivalent control is computed:

$$u_{eq} = -0.85 \mathbf{x}_1 + 0.2 \frac{(1 - \tau)}{\tau} \mathbf{x}_2.$$

From (20), it is possible to determine that over the switching surface:  $\mathbf{x}_2 = \frac{y_{ss} - \mathbf{x}_1}{\tau}$ ; consequently over the switching surface the equivalent control becomes:

$$\bar{u}_{eq} = \left( -0.85 - 0.2 \frac{1 - \tau}{\tau^2} \right) \mathbf{x}_1 + 0.2 \frac{(1 - \tau)}{\tau^2} y_{ss}.$$

The bounds for  $R$  are obtained by equaling  $u_{eq} = \pm 1$ , so:

$$\frac{-5\tau^2 - y_{ss}\tau + y_{ss}}{\frac{17}{4}\tau^2 - \tau + 1} \leq \mathbf{x}_1 \leq \frac{5\tau^2 - y_{ss}\tau + y_{ss}}{\frac{17}{4}\tau^2 - \tau + 1}.$$

Which for  $\tau = 0.5$  and  $y_{ss} = 0.75$  becomes:

$$-0.56 \leq \mathbf{x}_1 \leq 1.04. \quad (22)$$

Consequently, sliding regime will exist around the desired operation point  $y = \mathbf{x}_1 = y_{ss} = 0.75$ .

In Figure 7, it can be seen the SMCITOOL output for the case under study when initial conditions  $(\mathbf{x}_1(0), \mathbf{x}_2(0)) = (2, 0)$  are selected. As the initial conditions are outside the attraction zone in  $\pi^+$ , the trajectory hits the switching surface outside  $R$  so no sliding regime is produced (this corresponds to the first event). When crossing to  $\pi^-$ , the trajectory enters the attraction zone and after some time it hits the switching surface (second event) inside  $R$  and the sliding regime is produced. As the equivalent dynamics has been designed to be stable and the equilibrium point is inside  $R$ , the output asymptotically reaches  $y_{ss}$ .

As it can be seen in the left lower part, the control action begins equal to 1 because the trajectory begins in  $\pi^+$ , after the first event it turns into  $-1$ , and finally when the sliding regime begins the control action corresponds to the equivalent control.

In case the desired value for  $y$  changes from 0.75 to 1.25 implies that  $\mathbf{x}_1$  moves outside the range where the stability

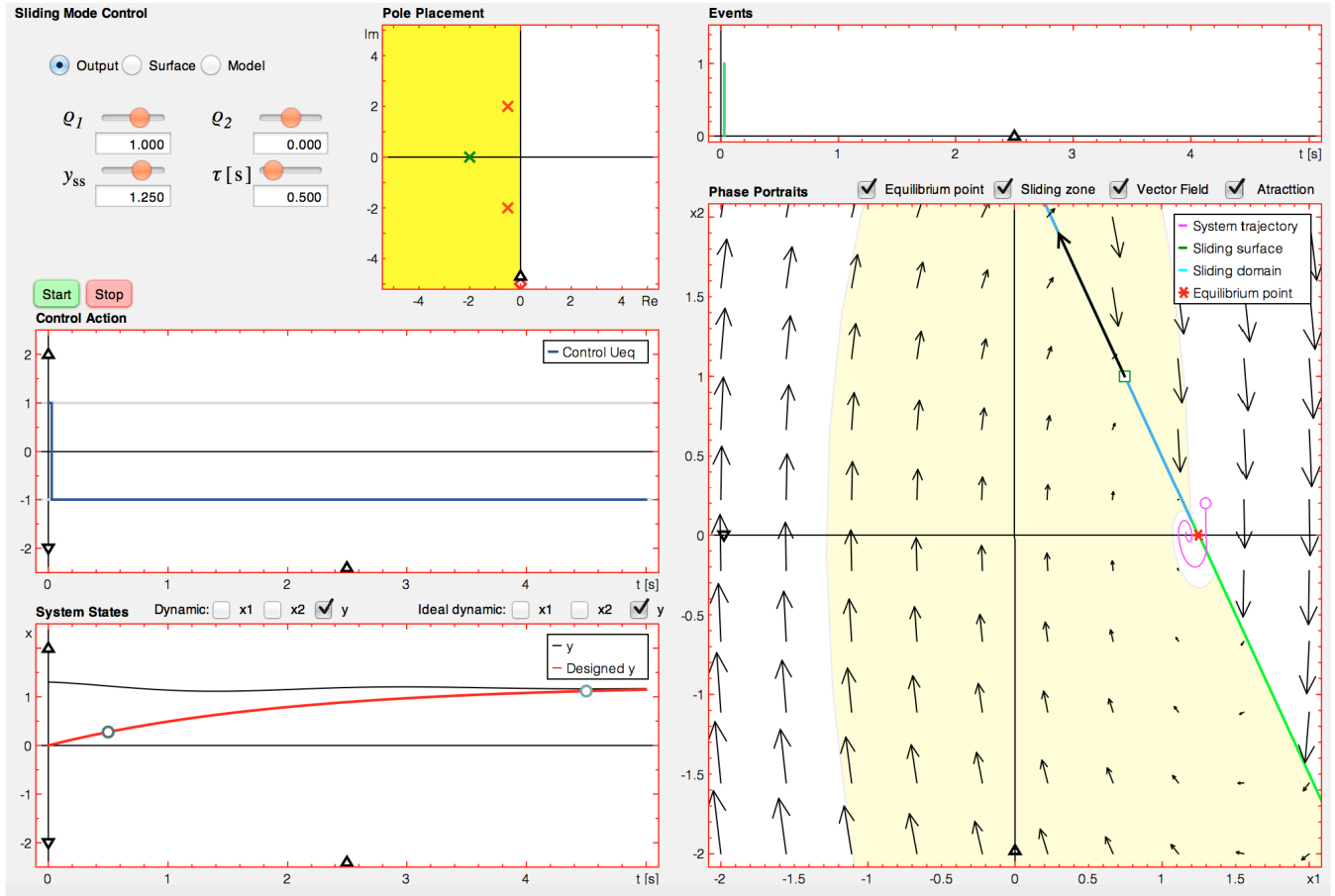


**FIGURE 8.** SMCITOOL: The view shows the case described in Example 1 for  $y_{ss} = 0.125$ . Trajectory begins in  $\pi^+$ , hits the sliding surface and enters  $\pi^-$ ; after some time it hits the sliding surface again and then enters the sliding regime. The trajectories lie over the sliding surface until the equivalent control reaches its lower limit, at this point another event is produced and trajectories return to  $\pi^-$  and converge to the equilibrium point of  $\dot{x} = f^-$ .

condition, (22), is fulfilled. This implies that the desired equilibrium point lies outside the region where sliding regime exist so the closed-loop system will not reach the desired point. Figure 8 shows the closed-loop evolution for this case. For the same initial conditions as in the previous case, trajectory hit the switching surface in a region where no sliding regime exist, thus the control action switches from 1 to  $-1$ . Finally, the trajectory reaches and equilibrium point in  $\pi^-$  which is different from the expected ( $y_{ss}$ ). Therefore, the designed control system does not fulfill the specifications.

## V. EXAMPLE 2

System (1) is defined by:

$$\mathbf{A} = \begin{pmatrix} 0 & 1 \\ 1.4 & -1.3 \end{pmatrix} \quad \mathbf{b} = \begin{pmatrix} 4 \\ 3 \end{pmatrix}.$$

and the control goal is to regulate the output:

$$y = \rho \mathbf{x} = [-0.53, -0.848] \mathbf{x}$$

to  $y_{ss} = -1.275$ .

This is an unstable linear system (the eigenvalues of  $\mathbf{A}$  are  $-2$  and  $0.7$ ) and the output relative degree is one ( $\rho \mathbf{b} \neq 0$ ). Consequently, it is only possible to regulate the value of  $y$  to

$y_{ss}$ . The switching surface is defined as ( $\gamma = \rho$ ,  $\delta = -y_{ss}$ ):

$$\sigma(\mathbf{x}) = \rho \cdot \mathbf{x} - y_{ss}. \quad (23)$$

In order to analyze the closed-loop behavior, firstly the transversality condition is analyzed:

$$(\nabla \sigma, \mathbf{b}) = -4.664 \neq 0.$$

Consequently, sliding regime might exist. Secondly, the equivalent control is obtained:

$$u_{eq} = -0.2545 \mathbf{x}_1 + 0.1227 \mathbf{x}_2.$$

Which over the switching surface becomes:

$$\bar{u}_{eq} = -0.33125 \mathbf{x}_1 - 0.14473 y_{ss}.$$

The bounds for the sliding region,  $R$ , can be obtained by solving  $\bar{u}_{eq} = 1$  and  $\bar{u}_{eq} = -1$ . From this, the sliding region corresponds to:

$$-3.0188 - 0.4369 y_{ss} < \mathbf{x}_1 < 3.0188 - 0.4369 y_{ss}.$$

Which for  $y_{ss} = -1.275$  is:

$$-2.4618 < \mathbf{x}_1 < 3.5759. \quad (24)$$

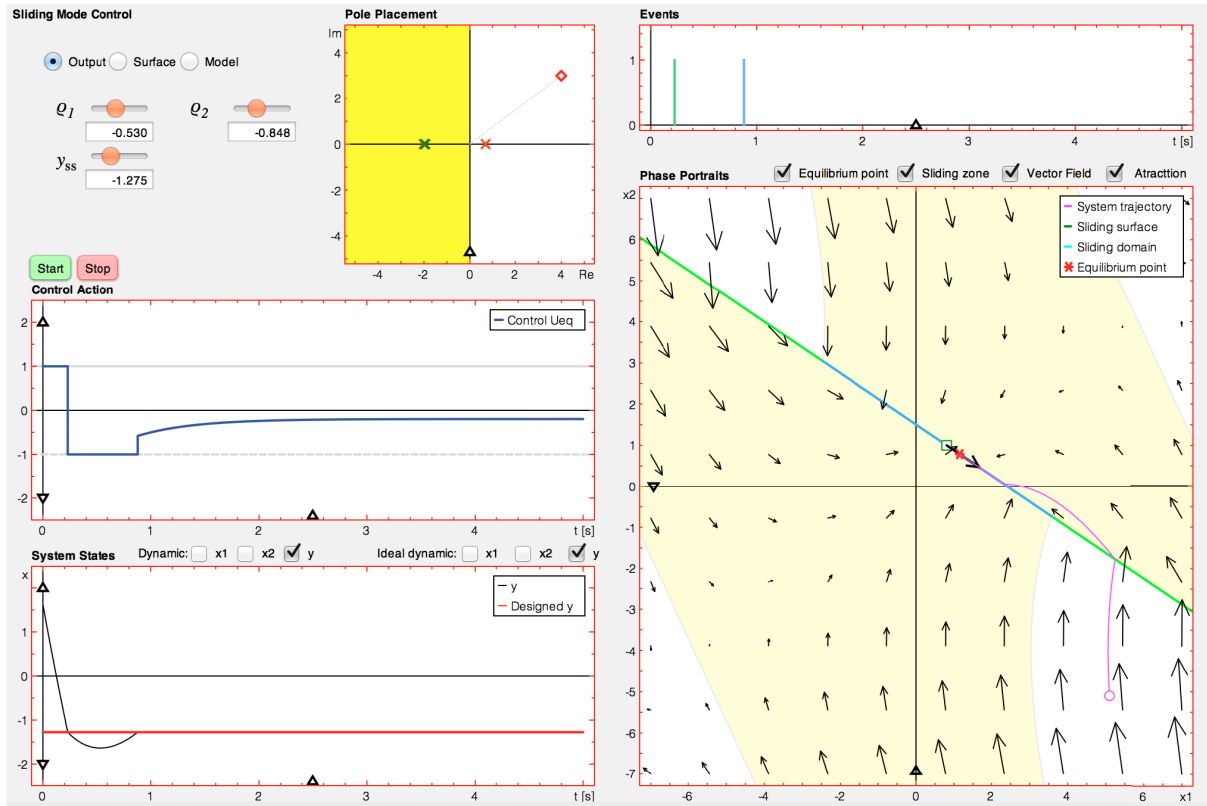


**FIGURE 9.** SMCITOOL: The view shows the case described in Example 2 for  $y_{ss} = -1.275$ . Trajectory begins in  $(5.1, 5.1)$  which is in the attraction zone of  $\pi^-$  so the trajectory hits the sliding surface in  $R$ . As the dynamics over the sliding surface is stable (the pole can be seen in green in the pole placement section) and the equilibrium point is in  $R$ , the output stays as  $y_{ss}$ . The state,  $x$ , converges asymptotically to the equilibrium point.

The dynamics over the switching surface, (10), can be written as:

$$\dot{\mathbf{x}}_1 = -1.95\mathbf{x}_1 - 1.7581 y_{ss},$$

which is a stable system with an equilibrium point at  $\mathbf{x}_1 = -0.9016 y_{ss}$ , which for  $y_{ss} = -1.275$  is 1.14956 which is inside the interval defined in (24). As a consequence a stable sliding regime will exist is the control goal will be achieved.

Figure 9 shows the SMCITOOL output for the case under study and  $y_{ss} = -1.275$  with initial conditions  $(\mathbf{x}_1(0), \mathbf{x}_2(0)) = (5.1, -5.1)$  placed in  $\pi^+$ . As the initial conditions are outside the attraction zone in  $\pi^+$ , after some time the trajectory hits the sliding surface outside  $R$ , but this time the trajectory is inside the attraction zone in  $\pi^-$ . After certain time the trajectory will hit  $R$  and as the equivalent dynamics is stable and the equilibrium point is in  $R$ , the trajectory remains in  $R$ . It is important to mention that in this case the system converges to the desired equilibrium point in finite time. As it can be seen in the lower left part of Figure 9, although  $y$  reaches  $y_{ss}$  in finite time, the states converge asymptotically to the equilibrium point.

## VI. CONCLUSIONS

In this work a methodology to introduce most relevant concepts behind sliding mode control has been presented. The methodology is almost self-contained and it does not assume any prior knowledge about the topic.

Planar sliding mode control has a very rich graphical representation, to take profit from this, a completely graphic and interactive tool has been designed to support the design and teaching duties. This tool uses an efficient event-based simulation approach which computes the solution trajectory very fast making it possible to interact with it. This tool allows to introduce students and designers to complex concepts in a simple and intuitive manner.

One of the functionalities of this tool is to determine the region of attraction of the sliding region. It is computed using an original methodology described in the paper.

Finally a couple of examples, have been included, to show how this tool can be used to analyze and design SMC planar systems.

## REFERENCES

- [1] R. Venkataraman, A. Šabanović, and S. Cuk, "Sliding mode control of dc-to-dc converters," in *Proc. IECON*, 1985, pp. 251–258.
- [2] N. F. Al-Muthairi and M. Zribi, "Sliding mode control of a magnetic levitation system," *Math. Problems Eng.*, vol. 2004, no. 2, pp. 93–107, 2004, doi: [10.1155/S1024123X04310033](https://doi.org/10.1155/S1024123X04310033).
- [3] V. Utkin, J. Guldner, and M. Shijun, "Sliding mode control in electro-mechanical systems," in *Automation and Control Engineering*. Boca Raton, FL, USA: CRC Press, 1999.
- [4] S. U. Din, Q. Khan, U.-R. Fazal, and R. Akmeliawanti, "A comparative experimental study of robust sliding mode control strategies for underactuated systems," *IEEE Access*, vol. 5, pp. 10068–10080, 2017.
- [5] H. Sira-Ramírez, "Differential geometric methods in variable structure control," *Int. J. Control*, vol. 48, no. 4, pp. 1359–1390, 1988.

- [6] J. J. Slotine and W. Li, *Applied Nonlinear Control*. Englewood Cliffs, NJ, USA: Prentice-Hall, 1991.
- [7] V. L. Utkin, *Sliding Modes and Their Application in Variable Structure Systems*. Moscow, Russia: MIR, 1978.
- [8] S. Spurgeon and C. Edwards, *Sliding Mode Control, Theory and Applications*. New York, NY, USA: Taylor & Francis, 1998.
- [9] J. M. Díaz, R. Costa-Castelló, R. Muñoz, and S. Dormido, "An interactive and comprehensive software tool to promote active learning in the loop shaping control system design," *IEEE Access*, vol. 5, pp. 10533–10546, 2017.
- [10] S. Dormido, S. Dormido, R. Dormido, and J. Sánchez, and N. Duro, "The role of interactivity in control learning," *Int. J. Eng. Edu.*, vol. 21, no. 6, pp. 1122–1133, 2005.
- [11] J. L. Guzmán, M. Berenguel, and S. Dormido, "Interactive teaching of constrained generalized predictive control," *IEEE Control Syst. Mag.*, vol. 2, no. 25, pp. 52–66, Dec. 2005.
- [12] J. L. Guzmán, R. Costa-Castelló, S. Dormido, and M. Berenguel, "An interactivity-based methodology to support control education: How to teach and learn using simple interactive tools [lecture notes]," *IEEE Control Syst.*, vol. 36, no. 1, pp. 63–76, Feb. 2016.
- [13] J. L. Guzmán, K. J. Aström, S. Dormido, T. Hägglund, and Y. Piguet, "Interactive learning modules for PID control," *IFAC Proc. Vols.*, vol. 39, no. 6, pp. 7–12, 2006.
- [14] N. Carrero, R. Costa-Castelló, S. Dormido, and E. Fossas, "Using interactive tools to teach/learn sliding mode control," in *Proc. 49th IEEE Conf. Decision Control*, Atlanta, GA, USA, Dec. 2010, p. 2.
- [15] J. L. Guzman, S. Dormido, and M. Berenguel, "Interactivity in education: An experience in the automatic control field," *Comput. Appl. Eng. Edu.*, vol. 21, no. 2, pp. 360–371, 2013.
- [16] S. Dormido, "Control learning: Present and future," *Annu. Rev. Control*, vol. 28, no. 1, pp. 115–136, 2004.
- [17] J. L. Guzman, K. J. Astrom, S. Dormido, T. Hagglund, M. Berenguel, and Y. Piguet, "Interactive learning modules for PID control [lecture notes]," *IEEE Control Syst.*, vol. 28, no. 5, pp. 118–134, Oct. 2008.
- [18] R. Sanchis, A. Julio Romero, and P. Balaguer, "Tuning of PID controllers based on simplified single parameter optimisation," *Int. J. Control*, vol. 83, no. 9, pp. 1785–1798, 2010.
- [19] J. M. Diaz, S. Dormido, and D. E. Rivera, "ITTSAE: A set of interactive software tools for time series analysis education [lecture notes]," *IEEE Control Syst.*, vol. 36, no. 3, pp. 112–120, Jun. 2016.
- [20] E. J. Normey-Rico, J. L. Guzman, S. Dormido, M. Berenguel, and F. E. Camacho, "An unified approach for DTC design using interactive tools," *Control Eng. Pract.*, vol. 17, no. 10, pp. 1234–1244, 2009.
- [21] G. C. Goodwin, S. F. Graebe, and M. E. Salgado, *Control System Design*, 1st ed. Upper Saddle River, NJ, USA: Prentice-Hall, 2000.
- [22] J. L. Guzmán Sánchez, R. Costa-Castelló, M. Berenguel Soria, and S. Dormido Bencomo, *Control Automático con Herramientas Interactivas*. London, U.K.: Pearson, 2012.
- [23] R. Longchamp, *Comande Numériques de Systèmes Dynamiques (Cours d'Automatique)*. Presses Polytechniques et Univ. Romandes, Lausanne, Switzerland, 2006.
- [24] F. E. Cellier and E. Kofman, *Continuous System Simulation*. New York, NY, USA: Springer, 2006. [Online]. Available: <http://www.springer.com/la/book/9780387261027>
- [25] *App Building*, MathWorks, Natick, MA, USA, 2016.
- [26] F. Esquembre, "Easy java simulations: A software tool to create scientific simulations in java," *Comput. Phys. Commun.*, vol. 156, no. 2, pp. 199–204, Jan. 2004.
- [27] Y. Piguet, *SysQuake 5: User Manual*, Calerga Sàrl, Lausanne, Switzerland, 2009.
- [28] H. K. Khalil, *Nonlinear Systems*. Englewood Cliffs, NJ, USA: Prentice-Hall, 2002.
- [29] A. F. Filippov, "Differential equations with discontinuous right hand sides," *Amer. Math. Soc. Transl.*, vol. 42, pp. 199–231, 1964. [Online]. Available: <https://bookstore.ams.org/trans2-42/>
- [30] F. E. Cellier, H. Elmqvist, M. Otter, and J. H. Taylor, "Guidelines for modeling and simulation of hybrid systems," *IFAC Proc. Vols.*, vol. 26, no. 2, pp. 1219–1225, 1993.
- [31] P. T. Piiroinen and Y. A. Kuznetsov, "An event-driven method to simulate filippov systems with accurate computing of sliding motions," *ACM Trans. Math. Softw.*, vol. 34, no. 3, 2008, Art. no. 13.
- [32] K. E. Brenan, S. L. Campbell, and L. R. Petzold, *Numerical Solution of Initial-Value Problems in Differential-Algebraic Equations*. Philadelphia, PA, USA: SIAM, 1996.



**RAMON COSTA-CASTELLÓ** (SM'07) received the B.S. degree in computer science from the Universitat Politècnica de Catalunya (UPC) in 1993 and the Ph.D. degree in computer science from the Advanced Automation and Robotics Program, UPC, in 2001. He is currently an Associate Professor with the Automatic Control Department (ESAI), UPC, and the Institut de Robòtica i Informàtica Industrial. His teaching activity is related to different aspects in automatic control. His research interests include the analysis and development of energy management (automotive and stationary applications) and the development of digital control techniques.

He is a member of CEA and IFAC (EDCOM, TC 9.4 Committee, and Automotive Control T.C. 7.1).



**NILIANA CARRERO** received the degree in system engineering from the University of the Andes, Venezuela, the master's degree in automatic control and robotics, and the Ph.D. degree in automatic control, robotics, and vision from the University of Catalonia, Spain, in 2006, 2010, and 2014, respectively. Her research interests include automatic control, modeling, and control for dc/dc power.



**SEBASTIÁN DORMIDO** (M'17) received the B.S. degree in physics from the Complutense University of Madrid, Spain, in 1968, the Ph.D. degree in physics from the University of the Basque Country, Leioa, Spain, in 1971, and the Honorary Doctorate degree from the University of Huelva and the University of Almería, Spain. In 1981, he was an appointed Professor of control engineering with National Distance Education University, Madrid. He has authored or co-authored over 250 technical

papers in international journals and conferences, and has supervised over 35 Ph.D. theses. His scientist activities include the computer control of industrial processes, model-based predictive control, hybrid control, and Web-based laboratories for distance education.

Dr. Dormido received the National Automatic Control Award from the IFAC Spanish Automatic Control Committee. From 2001 to 2006, he was the President of the Spanish Association of Automatic Control, CEA.



**ENRIC FOSSAS** (M'08) was born in Aiguafreda, Barcelona, Spain, in 1959. He received the degree in mathematics and the Ph.D. degree in mathematics from the Universitat de Barcelona, in 1981 and 1986.

In 1986, he joined the Department of Applied Mathematics, Universitat Politècnica de Catalunya (UPC), Barcelona, where he served as the head of the department from 1993 to 1999. In 1999, he moved to the Department of Automatic Control and Computer Engineering (ESAI) and to the Institute of Industrial and Control Engineering, as the Director of the Institute from 2003 to 2009. He is currently a Full Professor in control systems and automation. In 2013, he was appointed as a Rector of the UPC. His research interests include nonlinear control (theory and applications), particularly variable structure and hybrid systems, with applications to switching converters. He has authored/co-authored of over 100 scientific papers presented in conferences or published in specialized journals and of four books. He is member of the UPC Research Group Advanced Control on Energy Systems.

• • •